

BETA-DELAYED TWO-NEUTRON AND THREE-NEUTRON EMISSION

B. Jonson<sup>a)</sup>, H.Å. Gustafsson<sup>a)</sup>, P.G. Hansen<sup>b)</sup>, P. Hoff<sup>a)</sup>, P.O. Larsson<sup>c)</sup>, S. Mattsson<sup>c)</sup>, G. Nyman<sup>a)</sup>, H.L. Ravn<sup>a)</sup> and D. Schardt<sup>a)</sup>

- a) CERN-ISOLDE, CERN, Geneva, Switzerland
- b) Institute of Physics, University of Aarhus, Aarhus, Denmark
- c) Department of Physics, Chalmers University of Technology, Göteborg, Sweden.

Abstract

We review experiments on <sup>11</sup>Li that have led to the observation of two new radioactive decay modes: beta-delayed two- and three-neutron emission. The 2n decay mode was also observed in <sup>30,31,32</sup>Na and very recent results, reported for the first time here, show that it is detectable also in <sup>100</sup>Rb with  $P_{2n}/P_n = 0.027 \pm 0.007$ .

1. Introduction

Nuclear beta-decay to particle-unbound states may give rise to beta-delayed particle emission. The first example of this process was found in 1914 by Rutherford and Wood<sup>1)</sup> in experiments on naturally occurring thorium. They observed that some of the alpha particles had much higher energies than the main spectrum, and this finding was later explained by

Gamow<sup>2)</sup> as beta-delayed alpha emission. The first delayed neutrons were observed in 1939 in experiments<sup>3)</sup> on fission products produced in neutron bombardments of uranium. A new wave of interest in the field began in the early sixties<sup>4-9)</sup>, as may be seen from Table 1, and more than 100 precursors for delayed particle emission are now known. On-line mass separation has become increasingly important for the field and has promoted the process from being a barely detectable exotic nuclear decay mode to being an important tool in investigations of high-energy beta-decay. This evolution as well as the present state of the art are illustrated in contributions to the Cargèse Conference<sup>10,11)</sup> and to this conference<sup>12,13)</sup>.

In this paper we review the experiments on the two latest additions to Table 1: The beta-delayed two- and three- neutron precursors. The experiments have been carried out at the ISOLDE facility at CERN and at the on-line mass separator at the CERN PS. A summary of the results is given in Table 2.

Table 1

Delayed particle decay modes

Emitted particle	Reference	Year
Alphas	Rutherford and Wood <sup>1)</sup>	1916
Neutrons	Roberts et al. <sup>3)</sup>	1939
Protons	Karnaukhov et al. <sup>4)</sup> Barton et al. <sup>5)</sup>	1963
Fission	Skobolev <sup>6)</sup>	1972
Two neutrons	Azuma et al. <sup>7)</sup> Détraz et al. <sup>8)</sup>	1979
Three neutrons	Azuma et al. <sup>9)</sup>	1980

2. Experimental studies of beta-delayed two- and three-neutron emission

An inspection of nuclear mass tables<sup>14)</sup> shows that beta-delayed emission of more than one neutron (and also of more than one proton) becomes energetically possible very far from the region of beta stability. Figure 1 shows, as an example, the nuclear chart of the lightest elements with the expected precursors of beta-delayed two- and three-neutron emission indicated. One finds that an appreciable number of particle-stable nuclides are possible precursors. But in view of the fact that they all lie on the border regions that are hard to reach, it will be clear that the main experimental problems lie on the production side. For a detailed description of target-ion-source techniques, essential in this kind of work, the reader is referred to the

Table 2

Experimental branching ratios for beta-delayed two-neutron and three-neutron emitters

Isotope	$P_n$ (%)	$P_{1n}$ (%)	$P_{2n}$ (%)	$P_{3n}$ (%)	Ref.
<sup>11</sup> Li	95 ± 8	82 ± 7	3.9 ± 0.5	1.8 ± 0.2	9
<sup>30</sup> Na	a)	26 ± 4	1.2 ± 0.23	-	8
<sup>31</sup> Na	43 ± 11	-	1.0 ± 0.4	-	8
<sup>32</sup> Na	-	10 ± 4	5.1 ± 1.8 b)	-	8
<sup>100</sup> Rb	-	-	$P_{2n}/P_n = 2.7 \pm 0.7$	-	this work

a) See Section 2.3.

b) Weighted mean of neutron correlation and gamma measurement.

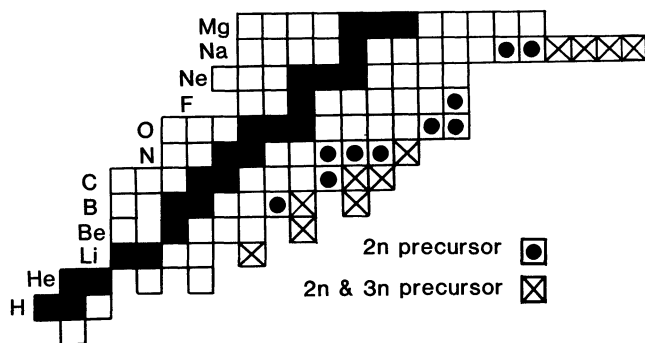


Fig. 1 Predicted precursors of beta-delayed two- and three-neutron emission in the lightest elements. The mass data used are taken from the tables of Wapstra and Bos<sup>14</sup>).

review paper by Ravn<sup>15</sup>). In the following we limit ourselves to a description of the experimental techniques used for the detection of the radiation.

## 2.1 Time-correlation measurements

2.1.1 Data-taking technique and strategy of data evaluation. The simultaneous emission of more than one neutron emitted after a beta decay to an excited nuclear state has been verified<sup>7-9</sup>) in neutron coincidence measurements. In these experiments the neutrons were detected with <sup>3</sup>He proportional counters embedded in a paraffin-wax moderator. Such a detector equipped with 12 neutron counters had an efficiency of  $\epsilon_n = 20 \pm 1\%$ . The beam of radioactivity was directed to a collector situated at the centre of the paraffin block. The residence time for a neutron emitted from this position was determined from  $\beta n$  coincidences on <sup>9</sup>Li. The time distribution was found to be exponential with a mean of  $\lambda^{-1} = 89 \pm 1 \mu s$ . This time is long compared to the response time of the <sup>3</sup>He detectors and it was therefore possible to connect all of them in parallel. In the string of neutron signals from the detector, neutron coincidences appear as time-correlated counts separated in time with a distribution characteristic of the residence time. The arrival times of the individual neutrons were recorded by feeding the neutron signals into a CAB microprocessor, which was used as a continuous time-to-digital converter recording the times of all the signals from the twelve <sup>3</sup>He tubes. The arrival times were recorded "on the fly" with a precision of 1  $\mu s$ . The correlation analysis was then performed in playback mode from magnetic tape.

The main problem in the analysis of the time-correlated data is to find the true rate of double and triple events in the presence of random correlations. As an example one may take <sup>11</sup>Li, which is a precursor of both two- and three-neutron emission: the random triple rate originates in this case in two sources: i) three single events combined to make a pure random triple event, and ii) a real double event detected together with a random single event. We shall in the following outline the main formulae for the rates of true and random events and also describe the strategy chosen in the analysis of our data.

Assume that we have a source with a total beta disintegration rate  $D$  and that it decays through channels involving the emission of  $i$  neutrons with

the probability  $p_{in}$  per beta decay<sup>\*</sup>). In most cases only a few of the neutrons from one event are registered and it is therefore convenient to define the rate of actual correlated events of  $s$  counts in the data string. If each multiplicity is characterized by an energy-independent average efficiency  $\epsilon_i$ , the rate of events with  $s$  neutrons detected is

$$R_s = D \sum_{i=s}^{\infty} p_{in}(i) \epsilon_i^s (1 - \epsilon_i)^{i-s}, \quad (1)$$

where  $\binom{i}{s}$  is the binomial coefficient. The quantities  $R_s$  are directly determined from a correlation analysis of the data and the ratios of the individual  $p_{in}$  values may be derived by solving Eq. (1).

In the actual data analysis a search for correlated events was done in a defined time interval  $\theta$  following an initial event. If  $(q - 1)$  neutrons are found within this time interval, the event is registered as  $q$ -fold. With the mean residence time for an event in the counter  $\lambda^{-1}$  the detection probability per unit time for an individual neutron belonging to the event is  $\lambda e^{-\lambda t}$ . The rate of true  $q$ -fold events found with such an analysis technique is

$$M_q^{(t)} = \sum_{s=q}^{\infty} R_s r_{s,q}, \quad (2)$$

where  $r_{s,q}$  is the probability that exactly  $(q - 1)$  events out of  $s - 1$  possible are falling inside the chosen time window

$$r_{s,q} = \binom{s-1}{q-1} (1 - e^{-\lambda\theta})^{q-1} e^{-\lambda\theta(s-q)} \quad (3)$$

The measured rate of  $q$ -fold events is with this strategy  $M_q = M_q^{(t)} + M_q^{(r)}$ , where  $M_q^{(r)}$  is the rate of random events. The random rate is dependent on the rate of registered neutrons and the corrections are calculated as combinations of events with lower multiplicity. The general formulae for the random rate become very complicated and we shall here only give those of interest in this work. In the case of doubles there is only one term given by the combination of two single events, (1)<sup>2</sup>,

$$M_2^{(r)} = R_1^2 \theta^2 e^{-R_1\theta}. \quad (4)$$

In the case of triples there are two types of random contributions. The first is a pure random triple event, that is of type (1)<sup>3</sup> which has the form

$$\frac{1}{2} R_1^3 \theta^2 e^{-R_1\theta}. \quad (5)$$

There are then three possible ways of combining a single event with a registered double event: i) a double registered first and then one single, ii) a single first, and iii) the single event registered in the time interval between the two events forming the double. The three terms are

$$(i) \quad R_1 R_2 \theta e^{-R_1\theta} \left[ 1 + \frac{(e^{-\lambda\theta} - 1)}{\lambda\theta} \right] \quad (6)$$

<sup>\*</sup>) Most formulae given here are not restricted to two- and three-neutron events but are generally valid for any multiplicity.

$$(ii) \quad R_1 R_2 \theta e^{-R_1 \theta} \left[ 1 - \frac{(1 - e^{-\lambda \theta})}{\lambda \theta} \right] \quad (7)$$

$$(iii) \quad R_1 R_2 \theta e^{-R_1 \theta} \left[ \frac{(1 - e^{-\lambda \theta})}{\lambda \theta} - e^{-\lambda \theta} \right] \quad (8)$$

From Eqs. (5) to (8) one then gets the total random triple rate as

$$M_3(r) = R_1 R_2 \theta e^{-R_1 \theta} \left\{ 2 - e^{-\lambda \theta} + \frac{(e^{-\lambda \theta} - 1)}{\lambda \theta} \right\} + \frac{1}{2} R_1^3 \theta^2 e^{-R_1 \theta} \quad (9)$$

### 2.1.2 Experimental results

**<sup>11</sup>Li.** The nuclide <sup>11</sup>Li is the only example of a precursor of both two- and three-neutron emission known to date. The decay scheme in Fig. 2 shows that its thresholds for 2n and 3n breakup lie as low as 7.315 MeV and 8.887 MeV, respectively<sup>16</sup>). The Q-value for the <sup>11</sup>Li β-decay is<sup>17</sup>) 20.7 MeV, which gives large energy-windows for the new decay modes. In the time-correlation measurement<sup>9</sup>) on <sup>11</sup>Li a uranium carbide target was used for the production of the activity<sup>15</sup>). The experiment was performed at different neutron count rates in order to check the random corrections. The change in the rate was obtained by varying the intensity of the 600 MeV proton beam from the CERN SC in an interval of 0.2 to 2 μA. The macrostructure of the beam was minimized by operating the cyclotron RF in the 1:1 mode corresponding to a 3 ms spacing between the beam pulses. This time is short in comparison with

the delay time in the target<sup>15</sup>) and the rate fluctuations due to the macrostructure of the proton beam may then be neglected. The long-term variations in the data rate  $D_n$  were corrected for by computing  $D_n$ ,  $D_n^2$ , and  $D_n^3$  for each buffer of about 1400 counts and by averaging over the whole time for the experiment. The biggest corrections (for the lowest data rate, 7.9 n/s) were found to be  $\langle D_n^2 \rangle / \langle D_n \rangle^2 = 1.011$  and  $\langle D_n^3 \rangle / \langle D_n \rangle^3 = 1.032$ .

The electronics system dead-time is 5 μs and the raw data had first to be corrected for the loss of events due to this. With a correlation time of  $\theta = 228$  μs this correction was 5.9% for doubles and 17.2% for triples.

The  $p_{2n}/p_{1n}$  and  $p_{3n}/p_{1n}$  ratios were derived from the dead-time-corrected raw data with the formulae given in Section 2.1.1. The assumption was made that  $\epsilon_i = \epsilon = 0.2$  for all multiplicities. Figure 3 shows the results as a function of the neutron singles count rate and one finds that there are no appreciable changes in the results due to this. The lower part of the figure illustrates that the results also remain stable within a wide range of chosen correlation-time intervals. The values adopted from these measurements are

$$p_{2n}/p_{1n} = (4.8 \pm 0.5) \times 10^{-2}$$

$$p_{3n}/p_{1n} = (2.2 \pm 0.2) \times 10^{-2}$$

These values combined with the total neutron emission probability,  $p_n = \sum_{i=1}^3 i p_{in}$  (Section 2.3) give the absolute values in Table 2.

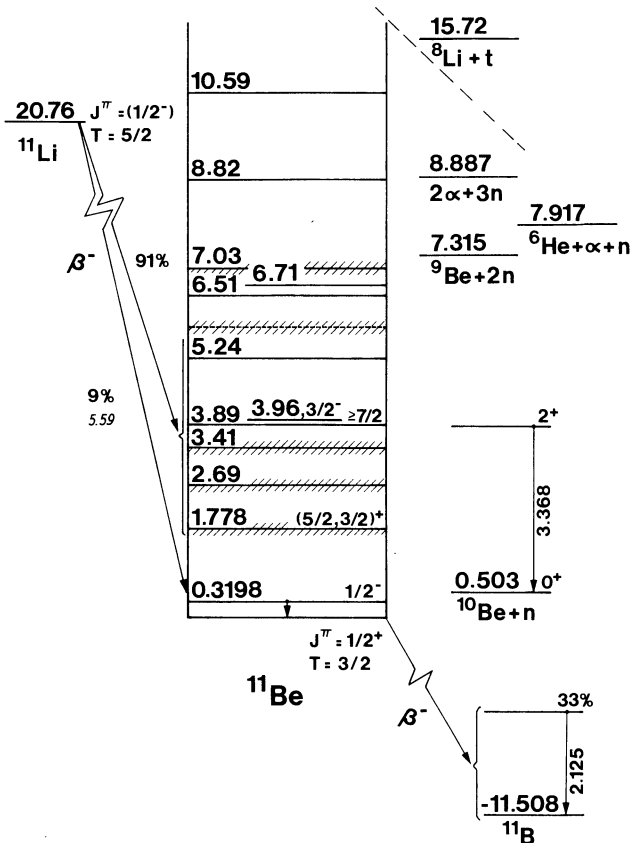


Fig. 2 Decay scheme of <sup>11</sup>Li (Ref. 12)

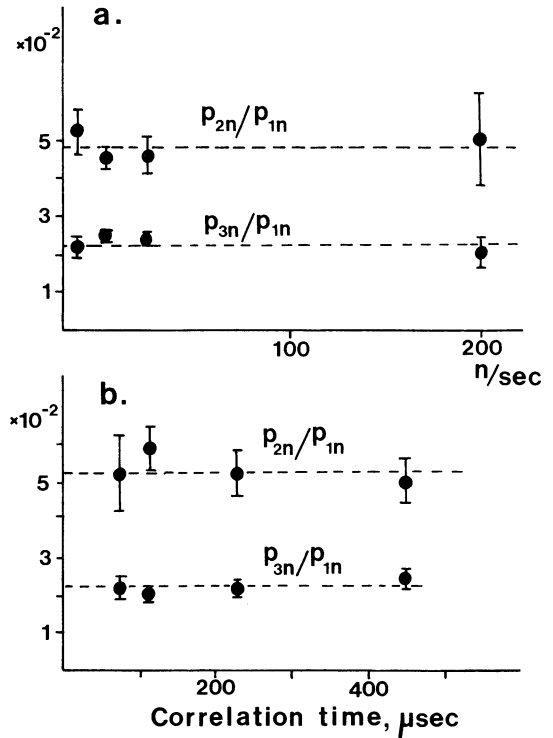


Fig. 3 a) Ratios of  $p_{2n}/p_{1n}$  and  $p_{3n}/p_{1n}$  for <sup>11</sup>Li as a function of the singles neutron rate in the experiment. b) Ratios of  $p_{2n}/p_{1n}$  and  $p_{3n}/p_{1n}$  for <sup>11</sup>Li with a singles neutron rate of 7.9 n/s obtained after correlation analysis with different choices of the correlation-time interval  $\theta$ .

The time-correlation curves in Fig. 4 show the distribution of the times between the first and the second neutron in cases where two or three neutrons are registered within the correlation interval. The time distribution, in the case of triples, is for the true events given by

$$R_3(t) dt = R_3 2\lambda e^{-2\lambda t} [1 - e^{-\lambda(\theta-t)}] dt \quad (10)$$

and for the random events by

$$R_{\text{rand}}(t) dt = \left\{ R_1 R_2 e^{-R_1 \theta} [(1 + e^{-\lambda t})(1 - e^{-\lambda(\theta-\lambda)}) + \lambda e^{-\lambda t}(\theta - t)] + R_1^3 e^{-R_1 \theta} (\theta - t) \right\} dt \quad (11)$$

The full drawn curves in Fig. 4 are calculated from these formulae using the results for  $R_1$  and  $R_2$  obtained from the data analysis. It is found that the results agree exactly with the calculated curves. From these results it can then be concluded that  $^{11}\text{Li}$  is a precursor both of beta-delayed two-neutron and three-neutron emission.

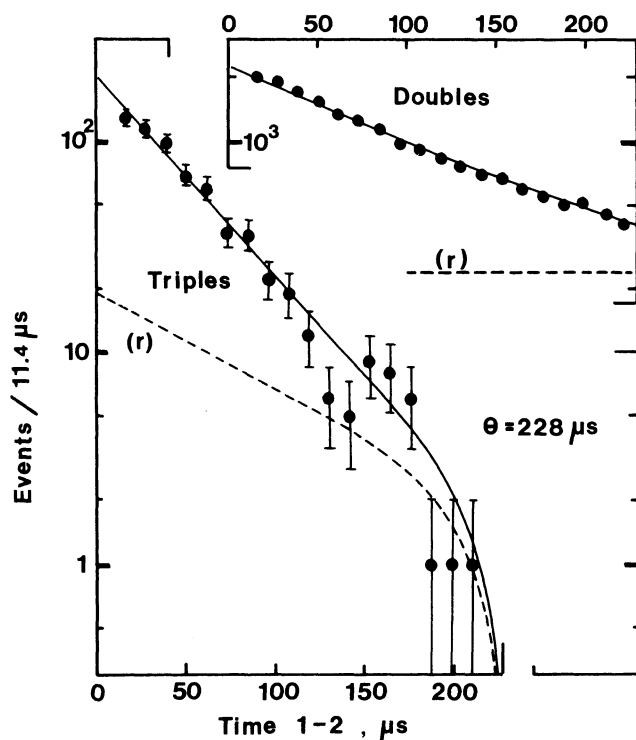


Fig. 4 Distribution of the time interval between the first and the second neutron for events registered as doubles and triples with a correlation time  $\theta = 228 \mu\text{s}$ . The data are from a 12 h experiment on  $^{11}\text{Li}$  with an average neutron rate of 22.9 counts/s. The theoretical curves have been calculated on an absolute scale from the correlation data and the formulae given in Eqs. (10) and (11).

$^{30-32}\text{Na}$ . Proton-induced fragmentation reactions in uranium targets give high yields of sodium isotopes out to mass 34. Since the lightest predicted precursor for beta-delayed two-neutron emission in sodium has mass 29 it is clear that this element gives interesting possibilities for studies of multi-neutron emission. Until now three of the sodium isotopes have been identified as precursors of two-neutron

emission (Table 2). The assignments have been made both in correlation measurements and in experiments with a gamma spectroscopic identification technique (Section 2.2).

The correlation measurement<sup>8)</sup> on sodium was made with a somewhat simpler system than that used for  $^{11}\text{Li}$ . Since the search was confined to observe two-neutron events, it was possible to use a 10 MHz clock that was started with a signal from the  $4\pi$  neutron counter. If a second neutron arrived within a pre-set time (6.55 ms) the clock was read. The counting rate had to be kept low to avoid distortion of the time spectrum. The results for  $^{30}\text{Na}$  and  $^{32}\text{Na}$  are shown in Fig. 5. The  $p_{2n}/p_n$  values obtained in these measurements were

$$^{30}\text{Na} : 0.042 \pm 0.008$$

$$^{31}\text{Na} : 0.023 \pm 0.005$$

$$^{32}\text{Na} : 0.24 \pm 0.05$$

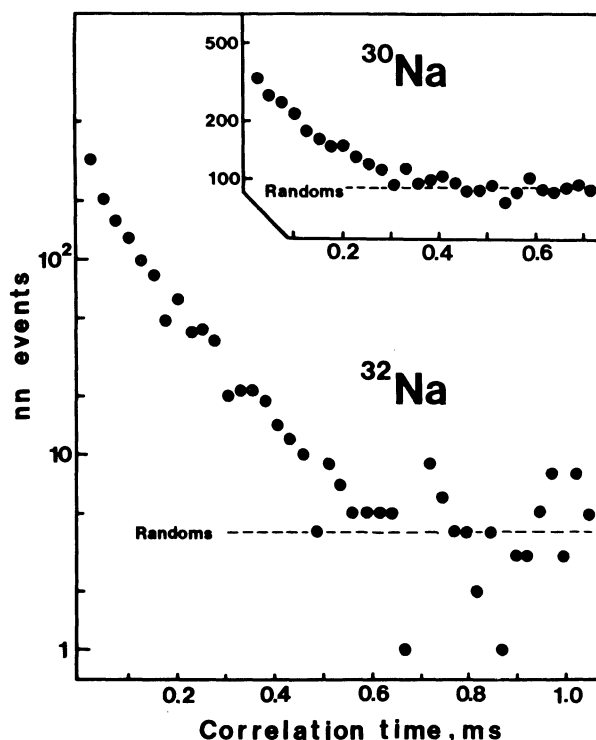


Fig. 5 Distribution of the nn time correlations for the isotopes  $^{30}\text{Na}$  and  $^{32}\text{Na}$ . The measuring time was 14.3 and 7.4 h, respectively. The high yield<sup>15)</sup> of  $^{30}\text{Na}$  made it necessary to reduce the initial beam intensity by a factor of 30 in order to cope with the random contribution (the dashed curves).

$^{100}\text{Rb}$ . Beta-delayed two-neutron emission from  $^{100}\text{Rb}$  was recently observed in an experiment at ISOLDE. The target system and the measuring equipment were of the same type as those used in the experiments on sodium. Several of the nuclides following the  $^{100}\text{Rb}$  decay are delayed-neutron precursors and the relative amount of the neutrons, detected at the mass setting 100, belonging to the

$^{100}\text{Rb}$  branch was determined from an experiment performed in a multiscaling mode. The result obtained in an 8 h experiment with an average neutron rate of 4.9 counts/s is  $p_{2n}/p_n = 0.027 \pm 0.007$ .

## 2.2 Gamma spectroscopic identification of 2n emission

As described in detail in the paper by Détraz et al.<sup>8)</sup>, beta-delayed two-neutron emission from the two isotopes  $^{30}\text{Na}$  and  $^{32}\text{Na}$  has also been detected with a gamma spectroscopic technique. These experiments use a mass spectrometer at the CERN PS<sup>17)</sup>, and the mass-separated beam was directed to the end of a thin Al collection tube. At a given mass setting A, gamma-rays belonging to the mass chains (A - 1) and (A - 2) could be detected with a Ge(Li) detector and indicated the contribution of 1n and 2n processes. A possible background due to cross contamination in the mass spectrometer was found to be negligible by checking the spectrum in a mass position corresponding to a value in between the mass positions A and (A - 1). The gamma spectra were normalized to the total number of atoms by monitoring the beta radioactivity during collection and from counting Na ions before and after collection. The result for  $^{30}\text{Na}$  is shown in Fig. 6. The spectrum clearly shows lines belonging to  $^{28}\text{Al}$  and  $^{28}\text{Si}$ . Since the 2n daughter  $^{28}\text{Mg}$  has a comparatively long half-life ( $T_{1/2} = 21.1\text{h}$ ) the counting was in this case performed in a shielded counting position off-line after a 10 h collection period. No lines from the short-lived isotopes belonging to the mass chain 29 are therefore observed in this experiment. The isotope  $^{28}\text{Mg}$  is also the daughter after three-neutron emission from  $^{31}\text{Na}$ . A search for mass 28 gamma lines at mass position 31 gave a limit to the 3n branch<sup>18)</sup> of  $p_{3n} < 5 \times 10^{-4}$ .

The two-neutron emission probabilities obtained from these experiments were  $(1.15 \pm 0.25)\%$  for  $^{30}\text{Na}$  and  $(5.5 \pm 2.5)\%$  for  $^{32}\text{Na}$ . These values are in good agreement with those found from the neutron-correlation data (see Section 2.3).

## 2.3 Measurements of $p_n^*$ values

The branching ratios of beta-delayed emission of one and two neutrons from  $^{32}\text{Na}$  could, in the CERN PS experiment<sup>8)</sup>, directly be determined from the mass 31 and 30 gamma-rays recorded from the activity collected at mass setting 32. The branches obtained were  $p_{1n} = 0.10 \pm 0.04$  and  $p_{2n} = 0.055 \pm 0.025$ . The correlation experiment gave  $p_{2n}/p_n = 0.24 \pm 0.05$  and with  $p_n = (p_{1n} + 2p_{2n}) = 0.21$  one then obtains  $p_{2n} = 0.050 \pm 0.019$ . The agreement between the two methods is thus excellent.

Most measurements of neutron branching ratios have, however, been measured relative to a precursor with known branching ratio. The case selected for normalization in the measurements on alkalides has been  $^9\text{Li}$  and the  $p_n$  value was taken from the measurements of Chen et al.<sup>19)</sup>. A measurement of the gamma spectrum from  $^{11}\text{Li}$  showed, however, that the feeding<sup>20)</sup> to the first excited state in  $^{11}\text{Be}$  at 320 keV is only  $(9.2 \pm 0.7)\%$ . The 2.12 MeV line from the daughter nucleus  $^{11}\text{B}$  (see Fig. 2) is also present in the spectrum (Fig. 7) and from this one obtains a feeding to the non-neutron emitting states of  $(9 \pm 2)\%$ , which gives an upper limit of 2% to the  $^{11}\text{Be}$  ground state. This is in clear contradiction with the earlier deduced<sup>21)</sup>  $p_n$  value of  $(61 \pm 7)\%$ . The  $p_n$  values for both  $^9\text{Li}$  and  $^{11}\text{Li}$  were therefore checked in a new experiment<sup>20)</sup>. Simultaneous counting of betas and neutrons was made, but the main technique adopted was a  $\beta n$  coincidence experiment. The betas were detected in a 1 mm thick plastic detector placed in the centre of a  $4\pi$  paraffin moderated neutron counter. The beta-neutron time distribution was then recorded together with the

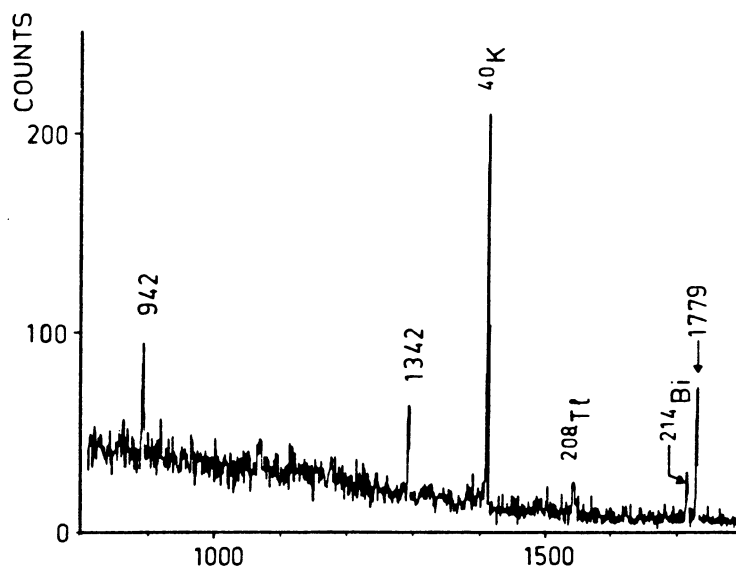


Fig. 6 Gamma spectrum measured after a 10 h collection of  $^{30}\text{Na}$ . The 942 keV and 1342 keV rays originate in the decay of the 21.1 h  $^{28}\text{Mg}$  and the 1779 keV ray in the decay of its daughter  $^{28}\text{Al}$ . These three lines were all absent in a spectrum measured on a sample collected in an intermediate mass position, which shows that their origin is in 2n emission and not in cross contamination from the separator.

\*) The total emission probability is defined as  $p_n = \sum_{i=1}^{\infty} i p_{in}$ , where a process leading to the emission of i neutrons is denoted  $p_{in}$ , so that  $\sum_{i=0}^{\infty} p_{in} = 1$ .

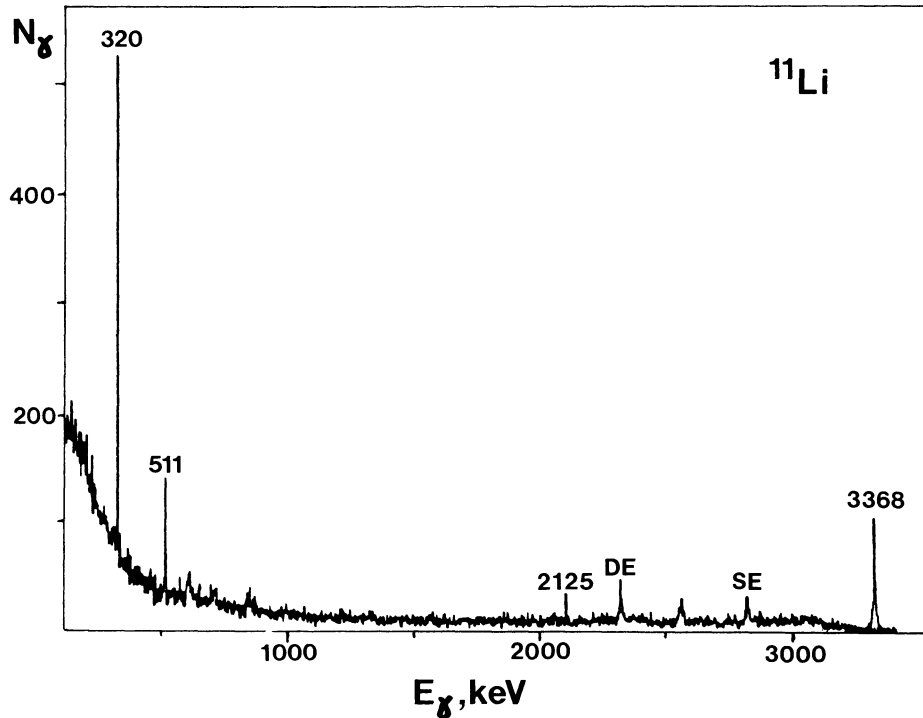


Fig. 7 Gamma spectrum from the  $^{11}\text{Li}$  beta decay. The lines at 320 keV and 2125 keV indicate that about 9% of the decay proceeds through the states that lie below the neutron-emission threshold. The line at 3.368 keV is from single neutron emission from the 3.89 MeV and 3.96 MeV states in  $^{11}\text{Be}$  to the  $2^+$  state in  $^{10}\text{Be}$  (see decay scheme in Fig. 2).

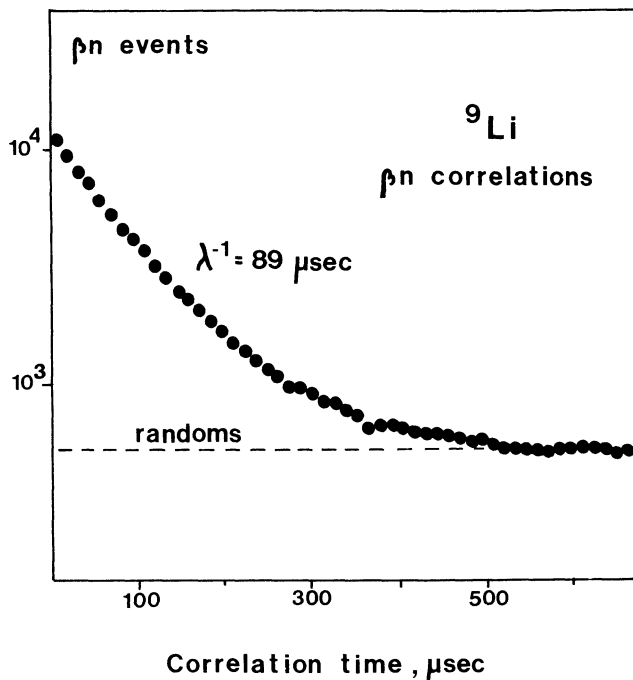


Fig. 8 The time distribution of  $\beta n$  events from the  $^9\text{Li}$  decay. The curve shows the slope typical of the neutron residence time in the detector with  $\lambda = 89 \mu\text{s}$ . The correlation data combined with data from simultaneous counting of neutrons and beta particles give a new value of the  $p_n$  value,  $p_n(^9\text{Li}) = 50 \pm 4\%$ .

singles rates. The spectrum in Fig. 8 shows the result for  $^9\text{Li}$  and one finds that the resulting time curve is typical of the neutron residence time in the counter system. The number of coincidences between betas and neutrons  $n_{\beta\gamma}$  is with this system

$$n_{\beta\gamma} = p_n \epsilon_n n_\beta, \quad (12)$$

where  $n_\beta$  is the beta rate and  $\epsilon_n$  the detector efficiency. The  $p_n$  value derived from these data is  $(50 \pm 4)\%$ . This value is much higher than the earlier value<sup>19)</sup> of  $(35 \pm 3)\%$ . The same set-up gave for  $^{11}\text{Li}$  a  $p_n$  value of  $(96 \pm 8)\%$ . The latter value combined with results from gamma measurements and values obtained relative to the  $^9\text{Li}$  value gave all values consistent with this result. The value adopted in Ref. 20 for the total emission probability of beta-delayed neutrons from  $^{11}\text{Li}$  is

$$p_n(^{11}\text{Li}) = \sum_{i=1}^3 p_{in} = (95 \pm 8)\%,$$

which gives the  $p_{in}$  values shown in Table 2. The new  $p_n$  value for  $^9\text{Li}$  gives a renormalization of a number of earlier published delayed-neutron branching ratios<sup>21,22)</sup>. For completeness we give in Table 3 a list of the readjusted branching ratios. One notes here that the new  $p_n$  value for  $^{30}\text{Na}$  does not agree with the  $p_{in}$  value obtained from the gamma counting<sup>23)</sup> when combined with the measured ratio  $p_{2n}/p_n$ . Until this discrepancy is cleared up we have in Table 2 adopted the value from Détraz et al.<sup>23)</sup>  $(26 \pm 4)\%$  for  $p_{1n}$ .

Table 3

Renormalized  $p_n$  values (%)

$^{11}\text{Li}$ a)	87	$\pm 10$
$^{27}\text{Na}$ a)	0.11	$\pm 0.04$
$^{28}\text{Na}$ a)	0.8	$\pm 0.2$
$^{29}\text{Na}$ a)	22	$\pm 3$
$^{30}\text{Na}$ a)	47	$\pm 5$
$^{31}\text{Na}$ a)	43	$\pm 11$
$^{93}\text{Rb}$ b)	1.8	$\pm 0.2$
$^{94}\text{Rb}$ b)	12.1	$\pm 1.3$
$^{95}\text{Rb}$ b)	12.2	$\pm 1.3$
$^{96}\text{Rb}$ b)	19	$\pm 2$
$^{97}\text{Rb}$ b)	39	$\pm 4$
$^{98}\text{Rb}$ b)	19	$\pm 3$
$^{145}\text{Cs}$ b)	17	$\pm 2$
$^{146}\text{Cs}$ b)	20	$\pm 2$

a) From Ref. 21.

b) From Ref. 22.

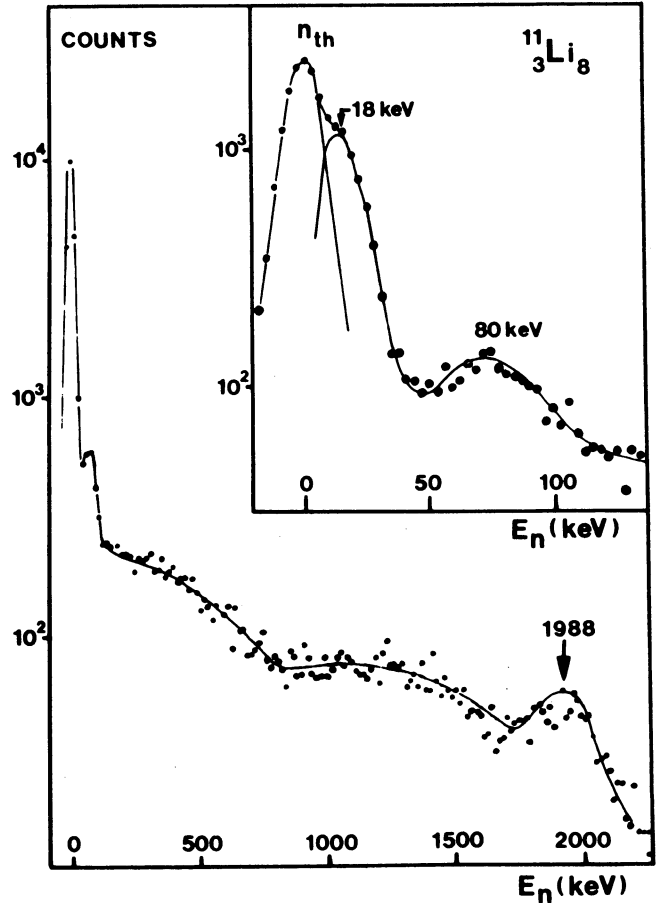


Fig. 9 Energy spectrum of delayed neutrons from  $^{11}\text{Li}$ . The lines at 18 keV and 80 keV shown in the inset originate in single-neutron emission to the  $2^+$  state in  $^{10}\text{Be}$  from the states at 3.89 MeV and 3.96 MeV in  $^{11}\text{Be}$ , respectively. The broad peak at about 1988 keV is from single-neutron emission connecting the 2.69 MeV state with the  $^{10}\text{Be}$  ground state. The continuum from about 100 keV and up to 1.6 MeV is most likely due to two-neutron and, to some extent, three-neutron emission.

#### 2.4 The energy spectrum of delayed neutrons from $^{11}\text{Li}$

An early indication<sup>25)</sup> of multi-neutron emission from  $^{11}\text{Li}$  was given by the neutron energy spectrum shown in Fig. 9. This spectrum, measured with three  $^3\text{He}$  spectrometers coupled in parallel, shows in addition to three broad lines, that can be interpreted as arising from neutron emission from known levels in  $^{11}\text{Be}$ , a broad continuum of neutron events. The shape of this part of the spectrum has a central minimum and it extends in energy up to about 1.6 MeV. Both these findings are consistent with an interpretation of the continuum as due to two-neutron emission from the 8.82 MeV state in  $^{11}\text{Be}$  to the ground state of  $^9\text{Be}$ . One knows further<sup>26)</sup> from the strong population of the 8.82 MeV state in the reaction  $^9\text{Be}(t,p)^{11}\text{Be}^*$  that there is a strong overlap between this state and the  $^9\text{Be}$  ground state + two neutrons. These observations provide good arguments that a large fraction of the observed continuum may originate in 2n emission from the 8.82 MeV state. The spectrum is, however, measured in singles mode and one has thus a contribution from the  $^{11}\text{Li}$  3n branch. To clear up the exact distributions from the different branches one has to design an experiment where they may be recorded independently. Such a measurement has to be made to the lowest possible energy since the broad ( $\Gamma = 200 \pm 50$  keV) 8.82 MeV state extends above the 3n threshold. Part of the 3n branch may come from this part of the resonance and the emitted neutrons would evidently be of very low energy. There is also a contribution to the 3n branch from neutrons emitted from states above the 8.82 MeV state. This has been shown in a study of the energy spectra of the two alpha particles, from the  $^8\text{Be}$  breakup, accompanying the three-neutron emission process<sup>24)</sup>. The charged-particle emission from the  $^{11}\text{Li}$  decay is discussed in the next section.

#### 2.5 Charged-particle emission following the $^{11}\text{Li}$ beta decay

In the beta-delayed three-neutron process the excited  $^{11}\text{Be}$  nucleus actually breaks up into five nuclear particles: three neutrons and two alpha particles. An alternative, indirect method to detect the presence of a three-neutron branch is therefore to search for the emitted alphas. Such an experiment has been performed<sup>24)</sup>, and in order to be sure that the origin of the particles was in  $^8\text{Be}$  they were measured in coincidence. The spectrum, constructed from the sum of the energies of the two alphas belonging to each event, is shown in Fig. 10. The  $p_{3n}$  value obtained from these data was found to be  $(2.3 \pm 0.6)\%$ , which is in good agreement with the result from the correlation analysis. The high-energy part of the spectrum can, as discussed in Ref. 24, only originate in beta feedings to states at excitation energies around 18.5 MeV in  $^{11}\text{Be}$ . The beta branch to this energy would then be about 0.3%,

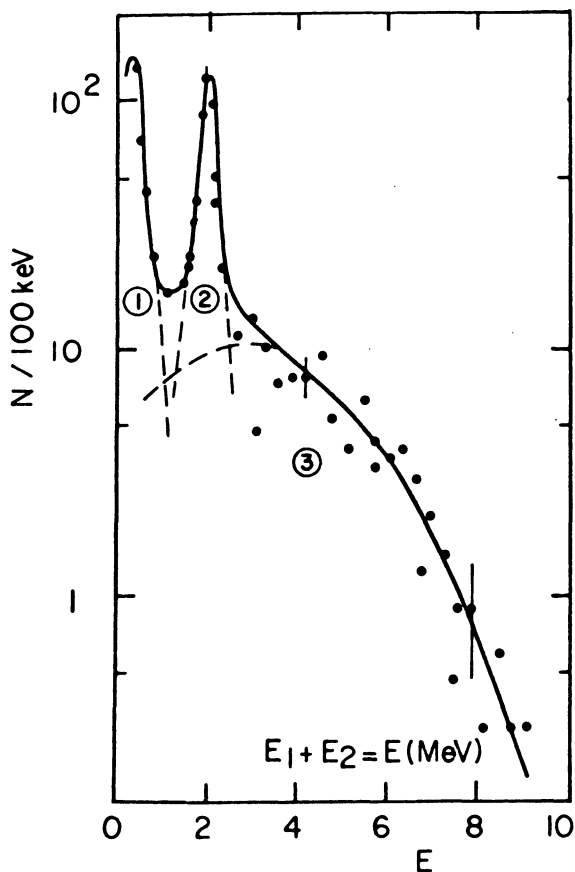


Fig. 10 Energy spectrum of the summed charged-particle coincidences from the  $^{11}\text{Li}$  decay. The three parts of the spectrum are in Ref. 24 interpreted as alpha-alpha coincidences after three-neutron emission (regions 1 and 3) and alpha- $^6\text{He}$  coincidences (region 2).

which would indicate a log ft value around 3.1 for this strength. The time-of-flight spectra for the charged particles were also recorded<sup>24)</sup> and from these there are indications that the single neutron branch from  $^{11}\text{Li}$  may be accompanied by  $^6\text{He}$  nuclei formed after the breakup:  $^{11}\text{Be}^* \rightarrow ^6\text{He} + \alpha + n$ .

### 3. Calculations of $p_{in}$ values

The gross theory of beta-decay has been applied in calculations of delayed-neutron branching ratios (Refs. 27-29). An extension of such calculations to include also two neutron branching ratios was made in Ref. 8. The general agreement between these calculations and the measured  $p_{2n}/p_n$  values for sodium was very good. We outline here the main features of these calculations with a recent extension<sup>30)</sup> to neutron multiplicities of order three.

The emission of neutrons is assumed to dominate over gamma de-excitations at an energy  $\delta$  above the neutron separation energy  $S_n$ . The beta-feed  $\beta(E)$  to the excitation energy  $E$  in the daughter nucleus, with mass  $A$ , is calculated from the gross theory. The giant resonance is assumed to have a modified Lorentz shape. The branching ratio for the emission of  $i$  neutrons is then given by the expression

$$p_{in} = \frac{\int_{S_{in}+\delta}^Q \pi_i(E)\beta(E) dE}{\int_0^Q \beta(E) dE} \quad (13)$$

The factor  $\pi_i(E)$  in the different parts of the excitation spectrum is given in Table 4, where

$$p_2 = \frac{\int_{S_{2n}+\delta}^{E-\delta} \Gamma_n(E, E_1)\rho(E_1 - S_{1n}) dE_1}{\int_{S_{1n}}^{E-\delta} \Gamma_n(E, E'_1)\rho(E'_1 - S_{1n}) dE'_1} \quad (14)$$

and

$$p_3 = \frac{1}{\int_{S_{1n}}^{E-\delta} \Gamma_n(E, E'_1)\rho(E'_1 - S_{1n}) dE'_1} \times \int_{(S_{3n}+2\delta)}^{E-\delta} \left\{ \Gamma_n(E, E_1)\rho(E_1 - S_{1n}) \times \int_{S_{3n}+\delta}^{E_1-\delta} \Gamma(E, E_1)\rho(E_1 - S_{2n}) dE_2 \right\} dE_1 \times \int_{S_{2n}}^{E_1-\delta} \Gamma(E_1, E'_2)\rho(E'_2 - S_{2n}) dE'_2 \quad (15)$$

Table 4

The factor  $\pi_i(E)$  used in Eq. (13)

Energy interval	$\pi_1(E)$	$\pi_2(E)$	$\pi_3(E)$
$0 < E \leq S_{1n} + \delta$	0	0	0
$S_{1n} + \delta < E \leq S_{2n} + 2\delta$	1	0	0
$S_{2n} + 2\delta < E < S_{3n} + 3\delta$	$1 - p_2$	$p_2$	0
$S_{3n} + 3\delta < E < Q$	$1 - p_2$	$p_2 - p_3$	$p_3$

If the parent nucleus has  $Z$  and  $A$  as charge and mass, respectively, the widths and level densities are in

$$\begin{aligned} \Gamma(E, E_1) &: (Z + 1, A) \\ \Gamma(E_1, E_2) &: (Z + 1, A - 1) \\ \rho(E_1 - S_{1n}) &: (Z + 1, A - 1) \\ \rho(E_2 - S_{2n}) &: (Z + 1, A - 2) \end{aligned} \quad (16)$$

The level density and the neutron width were calculated from the formulae given in Ref. 29. In the calculations the parameter  $\delta$  was chosen to be 50 keV. The resulting  $p_n$  values for some of the precursors in Na and Rb are shown in Table 5. One finds a good general agreement between the data and the results from this simple model.



Table 5

Calculated and measured half-lives and neutron branching ratios for multi-neutron precursors in sodium and rubidium

Isotope	Mass data used in the calculation				$T_{1/2}$ (ms)		$p_{1n}$		$p_{2n}/p_n$		$p_{3n}/p_n$	
	Q	$S_{1n}$	$S_{2n}$	$S_{3n}$	Exp.	Theor.	Exp.	Theor.	Exp.	Theor.	Exp.	Theor.
$^{30}\text{Na}$	18.18	7.12	10.92	> 18.18	53	60	0.26(4)	0.13	0.042(8)	0.072	0	0
$^{31}\text{Na}$	14.51	2.18	9.29	13.09	17	96	a)	0.33	0.023(5)	0.0076	< $10^{-3}$	$6 \times 10^{-8}$
$^{32}\text{Na}$	19.3	7.06	9.24	16.36	14.5	42	0.10(4)	0.134	0.24(5)	0.21	a)	$9 \times 10^{-6}$
$^{98}\text{Rb}$	12.2	6.37	9.64	> 12.2	130	506	0.19(3)	0.086	$3.8(6) \times 10^{-3}$	$2.8 \times 10^{-3}$	0	0
$^{100}\text{Rb}$	13.55	5.84	9.40	> 13.55	58	168	a)	0.309	0.027(7)	0.015	0	0
$^{102}\text{Rb}$	14.63	5.60	8.81	> 14.63	a)	105	a)	0.39	a)	0.06	0	0

a) not measured.

The calculated one-neutron and two-neutron intensities as a function of the excitation energy for  $^{32}\text{Na}$  are shown in Fig. 11. One finds that the emission of two neutrons starts to dominate over one-neutron emission close above the threshold energy for two-neutron emission.

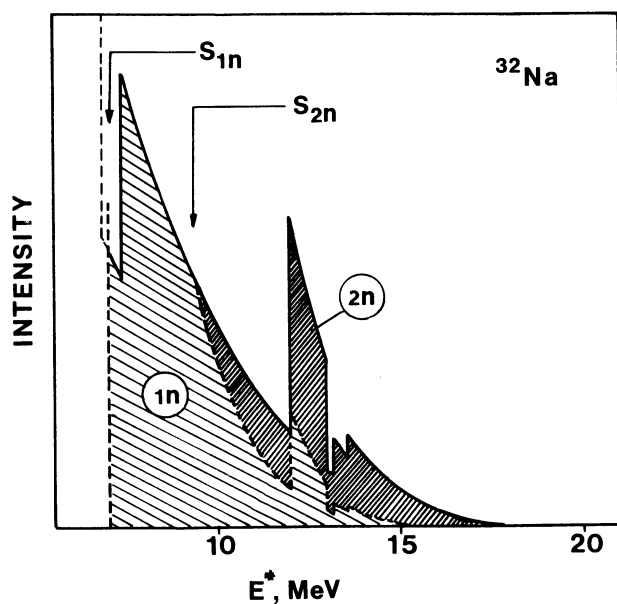


Fig. 11 Calculated  $^{32}\text{Na}$  delayed-neutron intensity as a function of the excitation energy in the  $^{32}\text{Mg}$  daughter. The calculated one- and two-neutron contributions are 13% and 4.5%, respectively, in excellent agreement with the experimental values. Note that the discontinuities in the spectrum arise from the schematic treatment of the pairing in the gross theory of beta decay. The calculation is entirely based on the parameters used in Ref. 30, so that no adjustment has taken place.

#### 4. Discussion

The studies of beta-delayed multi-neutron processes are still in their infancy. The experiments performed to date have, however, shown that the technique for the production of very neutron-rich nuclides has reached a level of sophistication where several precursors can be produced in comparatively high yields. This makes a number of detailed investigations possible in the years to come.

The most striking result obtained until now is maybe the strong  $p_{2n}$  branches observed in the sodium isotopes. In  $^{32}\text{Na}$ , for example, half of the emitted neutrons are from the two-neutron branch. The heaviest element for which two-neutron emission precursors have been identified is rubidium. The lightest isotope showing this decay mode<sup>31)</sup> is  $^{98}\text{Rb}$  and the  $p_{2n}/p_n$  ratio for  $^{100}\text{Rb}$  is as strong as 2.7%. These results show that the multi-neutron processes are not rare among nuclei far from stability, which means that they must play a significant role in the calculations of yields in the astrophysical r-process, since the branches become strong already for nuclei that lie much closer to stability than those in the r-process path.

The beta-delayed emission of two or three neutrons originates in the highest part of the excitation spectrum in the beta-decay daughter. The calculated one- and two-neutron contributions in the  $^{32}\text{Na}$  decay, illustrated in Fig. 11, show that two-neutron emission becomes the dominating decay mode at about 13 MeV excitation. The measured  $p_{2n}$  value therefore gives information about the integrated beta strength to this part of the spectrum. This feature gives the possibility of applying the measured  $p_{1n}$  data in the investigations of the beta-strength functions in nuclei very far from stability. A mapping of delayed two- and three-neutron branches, in different parts of the nuclear chart, would be an extremely useful test of our understanding of these phenomena.

## References

- 1) E. Rutherford and A.B. Wood, *Phil. Mag.* 31, 379 (1916).
- 2) G. Gamow, *Nature* 126, 397 (1930).
- 3) R.B. Roberts, R.C. Meyer and P. Wang, *Phys. Rev.* 55, 510 (1939).
- 4) V.A. Karnaukhov, G.M. Ter-Akopian and V.G. Subbotin *in Proc. Third Conf. on Reactions between Complex Nuclei, Asilomar, Pacific Grove, 1963* (University of California Press, Berkeley, 1963), p. 434.
- 5) R. Barton, R. McPherson, R.E. Bell, W.R. Frisken, W.T. Link and R.B. Moore (*Can. J. Phys.* 41, 2007 (1963)).
- 6) N.K. Skobolev, *Soviet J. Nucl. Phys.* 15, 249 (1972).
- 7) R.E. Azuma, L.C. Carraz, P.G. Hansen, B. Jonson, K.-L. Kratz, G. Mattsson, G. Nyman, H. Ohm, H.L. Ravn, A. Schröder and W. Ziegert, *Phys. Rev. Lett.* 43, 1652 (1979).
- 8) C. Détraz, M. Epherre, D. Guillemaud, P.G. Hansen, B. Jonson, R. Klapisch, M. Langevin, S. Mattsson, F. Naulin, G. Nyman, A.M. Poskanzer, H.L. Ravn, M. de Saint-Simon, K. Takahashi, C. Thibault and F. Touchard, *Phys. Lett.* 94B, 307 (1980).
- 9) R.E. Azuma, T. Björnstad, H.Å. Gustafsson, P.G. Hansen, B. Jonson, S. Mattsson, G. Nyman, A.M. Poskanzer and H.L. Ravn, *Phys. Lett.* 96B, 31 (1980).
- 10) J.C. Hardy, *Proc. Third Int. Conf. on Nuclei far from Stability, Cargèse, 1976, CERN 77-30* (1977), p. 267.
- 11) B. Jonson, E. Hagberg, P.G. Hansen, P. Hornshøj and P. Tidemand-Petersson, *Proc. Third Int. Conf. on Nuclei far from Stability, Cargèse, 1976, CERN 77-30* (1977), p. 277.
- 12) J.C. Hardy, these proceedings.
- 13) E. Roeckl, these proceedings.
- 14) A.H. Wapstra and K. Bos, *At. Data Nucl. Data Tables* 19, 175 (1977).
- 15) H.L. Ravn, *Phys. Rep.* 54, No. 3, 201 (1979).
- 16) F. Ajzenberg-Selove and C.L. Busch, *Nucl. Phys.* A336, 4 (1980).
- 17) C. Thibault, R. Klapisch, C. Rigaud, A.M. Poskanzer, E. Prieels, L. Lessard and W. Reisdorf, *Phys. Rev. C* 12, 644 (1975).
- 18) C. Détraz, D. Guillemaud, M. Langevin, F. Naulin, M. Epherre, R. Klapisch, M. de Saint-Simon, C. Thibault and F. Touchard, Abstract submitted to this conference, p. 63.
- 19) Y.S. Chen, T.A. Tombrello and R.W. Kavanagh, *Nucl. Phys.* A146, 136 (1970).
- 20) T. Björnstad, H.Å. Gustafsson, P.G. Hansen, B. Jonson, V. Lindfors, S. Mattsson, A.M. Poskanzer and H.L. Ravn, *Nucl. Phys.* A359, 1 (1981).
- 21) E. Roeckl, P.F. Dittner, C. Détraz, R. Klapisch, C. Thibault and C. Rigaud, *Phys. Rev. C* 10, 1181 (1974).
- 22) E. Roeckl, P.F. Dittner, R. Klapisch, C. Thibault, C. Rigaud and R. Prieels, *Nucl. Phys.* A222, 621 (1974).
- 23) C. Détraz, D. Guillemaud, G. Huber, R. Klapisch, M. Langevin, F. Naulin, C. Thibault, L.C. Carraz and F. Touchard, *Phys. Rev. C* 19, 164 (1979).
- 24) M. Langevin, C. Détraz, D. Guillemaud, F. Naulin, M. Epherre, R. Klapisch, S.K.T. Mark, M. de Saint-Simon, C. Thibault and F. Touchard,  $\beta$ -delayed charged particles from  ${}^9\text{Li}$  and  ${}^7\text{Li}$ , *Nucl. Phys. A*, in press.
- 25) R.E. Azuma, L.C. Carraz, P.G. Hansen, B. Jonson, K.-L. Kratz, S. Mattsson, G. Nyman, H. Ohm, H.L. Ravn, A. Schröder and W. Ziegert, *in Proc. Seventh Int. Workshop on Gross Properties of Nuclei and Nuclear Excitations, Hirschegg, Austria, 1979, (ed. H.V. Groote) (Technische Hochschule, Darmstadt, Germany, 1979), p. 132.*
- 26) F. Ajzenberg-Selove, R.F. Casten, O. Hansen and T.J. Mulligan, *Phys. Lett.* 40B, 205 (1972).
- 27) T. Kodama and K. Takahashi, *Nucl. Phys.* A239, 989 (1975).
- 28) K. Takahashi, *Prog. Theor. Phys.* 47, No. 5, 1500 (1972).
- 29) K. Takahashi, private communication.
- 30) K. Takahashi, M. Yamada and T. Kondoh, *At. Data Nucl. Data Tables* 12, 101 (1973).
- 31) P.L. Reeder, R.A. Warner, T.R. Yeh, R.E. Chrien, R.L. Gill, H. Lion, M. Schmid and M.L. Stelts, these proceedings.

## DISCUSSION

*J. Theobald:* For coincidence measurements it is not convenient to have the neutron-moderation time involved. One could instead record fast neutron-coincidences using a boron-10-plot ( $n, \alpha\gamma$ )-detector for low energetic neutrons and a proton-recoil plastic or liquid scintillator for high energetic neutrons. (You would have a neutron-energy blackout between about 30 keV and about 250 keV.)

*B. Jonson:* Thank you for the suggestion.

*G. Rudstam:* The formulas for the rate of s-fold events used as basis for the analysis are strictly valid only if the efficiency of detecting neutrons is constant. Did you measure the energy dependence of the efficiency of your neutron counter, and did you evaluate the possible effect of an energy dependence of  $\epsilon$  on your results? The neutron counter at Studsvik for example, has a quite pronounced energy dependence, but this will vary from detector to detector according to the amount of moderating material and the arrangement of the detector tubes.

*B. Jonson:* We have of course looked at the energy dependence found in your work but since the spectra in our case still are unknown, it is not possible to apply corrections. Our data are presented in a way so that corrections can easily be applied when the information becomes available.

*Ya. Gangrsky:* Are you going to measure the angular correlation of two neutrons?

*B. Jonson:* This would be interesting to do. Such data together with energy spectra for the individual branches (2n, 3n for  $^{11}\text{Li}$ ) could maybe give a clue to an understanding of the details of the decay process.

*K. Kratz:* You mentioned that the  $P_{2n}$ -value of  $^{100}\text{Rb}$  is about an order of magnitude higher than the value deduced from the gross theory of  $\beta$ -decay. According to the definition of the  $P_{2n}$  as the ratio of cumulative  $\beta$ -branches to certain energy ranges, the high experimental value may be taken as a first indication that a strong resonance in  $S_{\beta}(E)$  of  $^{100}\text{Sr}$  exists above the two-neutron binding energy. Such a resonance, centered around 9-10 MeV excitation energy, is also seen in  $^{95,96,97}\text{Rb}$ .

*B. Jonson:* With the Q-values shown in Table 5, I would say that the agreement is surprisingly good between this simple model and experiments.

*M. Langevin:* The decay scheme of  $^{11}\text{Li}^*$  can give an at least partial answer to the question whether the 2n and 3n decays are sequential or not. The neutron feeding of the 94 MeV excited level of  $^{10}\text{Be}$  can be identified by the  $\alpha$  decay part of this level. As about half of this decay proceeds by 2n emission, one can see that at least a great part of  $^{11}\text{Li}$  3n decay is sequential.

\*) Fig. 6 of our communication at this conference.

*B. Jonson:* If your suggested decay scheme is correct, I agree.